

COMPLEXITY ANALYSIS OF AN EDGE PRESERVING CNN SAR DESPECKLING ALGORITHM

*Sergio Vitale*¹, *Giampaolo Ferraioli*² and *Vito Pascazio*¹

¹ Dipartimento di Ingegneria, Università di Napoli Parthenope

²Dipartimento di Scienze e Tecnologie, Università di Napoli Parthenope

ABSTRACT

SAR images are affected by multiplicative noise that impairs their interpretations. In the last decades several methods for SAR denoising have been proposed and in the last years great attention has moved towards deep learning based solutions. Based on our last proposed convolutional neural network for SAR despeckling, here we exploit the effect of the complexity of the network. More precisely, once a dataset has been fixed, we carry out an analysis of the network performance with respect to the number of layers and numbers of features the network is composed of. Evaluation on simulated and real data are carried out. The results show that deeper networks better generalize on both simulated and real images.

Index Terms— SAR, despeckling, deep learning, CNN, denoising.

1. INTRODUCTION

The several decades of investment in earth observation has marked remote sensing as a very important topic where the research invest on.

SAR sensors acquire images continuously during day and night and are a useful tool for several tasks, such as monitoring, classification, segmentation etc. Unfortunately, SAR images are affected by a multiplicative noise called speckle that impairs their interpretation. The speckle is due to the coherent and incoherent interference among the backscatterings from the objects inside a single sensor resolution cell. Coherent interference (such as multiple bounces) are responsible of bright points while the dark points are results of incoherent interference. The resulting image of a SAR sensor is composed of an alternation of bright and dark points that get more difficult the interpretation [1].

This is the reason why a lot of research has been spending on the implementation of despeckling filters. Indeed, SAR despeckling is a key tool in the pre-processing chain of SAR image interpretation: actually denoising is fundamental for further task such as detection, classification, segmentation and 3D reconstruction [2], [3],[4].

Among all the filters there is a distinction in three main categories: local filters, non local (NL) filters and CNN based

filters. NL filters reach the State of the Art (SoA) performance thanks to the fact that they rely on the similarity among patches in all the images: such filters look for all the patches that are similar each other according to a certain criteria [5]. The difference between the NL filters is in the chosen similarity and combination criteria [6], [7],[8]. Thanks to this behaviour, they reach a large gain, mainly on edge preservation, respect to the local filters that combine only the adjacent pixel to the target one [1]. In the last years deep learning set a breakthrough in many fields of image processing such as classification, segmentation and detection reaching SoA performance [9]. This improvement lured attraction in all the research field and not less in the remote sensing society.

Several despeckling filters based on the use of convolutional neural network have been proposed such as [10], [11], [12], [13]. In our last proposal [12] and the improved version proposed in [14], we focused on the implementation of the cost function. Whereas, in this work we pay attention on the network's architecture, mainly on the number of layers and features extracted. Naturally, the complexity of the network and the dimension of the dataset are related each other, so we want to find out the upper bound for the complexity of the network (most number of layers and features) we can train and if deeper means better. So we train different networks with different depths and number features, and conduct an analysis of the results.

2. METHOD

In this work, we propose an analysis of the impact on the performance of the CNN complexity. We train different networks with different number of layers and features in order to find out the best depth and width of the network. We consider as baseline our network proposed in [14], that was a CNN of ten layers trained on simulated data.

2.1. Related Work

In [14], the simulation process was hold under the fully developed hypothesis: we simulate the speckle N with a Gamma

distribution $p(N)$ and number of look $L = 1$

$$p(N) = \frac{1}{\Gamma(L)} L^L N^{L-1} e^{-NL}$$

It means, we are considering the speckle backscattered by homogeneous areas. Once the speckle has been simulated, we multiple it to a noise-free image X in order to obtain a simulated SAR image $Y = X \cdot N$

In [14], we focus mainly on the definition of a cost function that take care of spatial and spectral properties of SAR images combining three terms

$$\begin{aligned} \mathcal{L} &= \mathcal{L}_2 + \lambda_{edge} \mathcal{L}_{edge} + \lambda_{KL} \mathcal{L}_{KL} \\ \mathcal{L}_2 &= \|\hat{X} - X\|^2 \\ \mathcal{L}_{edge} &= \left\| \left(\frac{\partial X}{\partial u} - \frac{\partial \hat{X}}{\partial u} \right)^2 + \left(\frac{\partial X}{\partial v} - \frac{\partial \hat{X}}{\partial v} \right)^2 \right\| \\ \mathcal{L}_{KL} &= D_{KL} \left(\frac{Y}{\hat{X}}, \frac{Y}{X} \right) = D_{KL}(\hat{N}, N) \end{aligned}$$

where X, \hat{X} and \hat{N} are respectively the noise-free reference, the estimated noise-free image and the estimated noise. The couple (u, v) indicate the horizontal and vertical direction of the image. \mathcal{L}_2 is the MSE between the reference and the estimated noise-free image. \mathcal{L}_{edge} is a measure of the difference of the gradient along the horizontal and vertical directions of X and \hat{X} . \mathcal{L}_{KL} is the Kullback-Leibler divergence (KLD) between the distributions of the estimated noise N and the theoretical one.

The first two terms are responsible of preserving spatial details and edges, respectively. The last one involves the estimated noise in order to preserve statistical properties of the SAR image. For a deeper insight and all the details of the method, the reader is invited to refer to [14].

2.2. Proposed Analysis

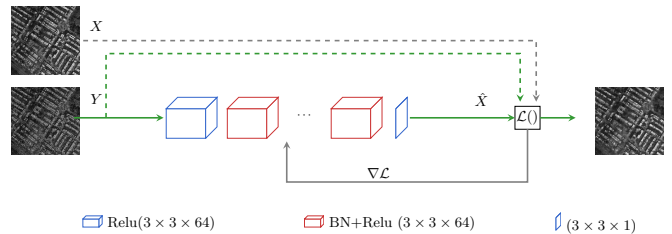
In this work we focus on the network architecture, more precisely on its depth and width: starting from the architecture proposed in [14], we train different networks with a fixed simulated dataset.

We consider the Merced Land Use dataset [15] and use $(57526 \times 64 \times 64)$ patches for training and $(14336 \times 64 \times 64)$ for validation.

In Fig.1, the basic architecture of the network is depicted. Generally each trained network is composed of a first convolutional layer with n_f features followed by a ReLU as activation function. Following, there are several inner convolutional layers with n_f followed by a ReLU as well, and by batch normalization. In the end, the last layer is a simple convolutional layer with a single output.

The kernel size ($K \times K$) of each convolutional layers is fixed to (3×3) . The number of layers varies from a minimum

Fig. 1: Baseline Network: it is composed of a first convolutional layer followed by ReLU, several inner convolutional layer followed by ReLU and batch Normalization and the output layer is a convolutional layer



of ten to a maximum of seventeen. We were not able to train deeper networks. For each network, we exploit the influence of extracted features, training the same architecture once with $n_f = 32$ features and once again with $n_f = 64$ features. Table 1 lists the architectures trained in this paper:

- $M\#_t$ stays for thin network trained with $n_f = 32$ features
- $M\#_1$ stays for large network trained with $n_f = 64$ features

Table 1: Architectures under test: network from 10 to 17 layers are considered. For each network ($M\#$) two versions are trained: a thin version with 32 layers ($M\#_t$) and a larger version with 64 features ($M\#_1$)

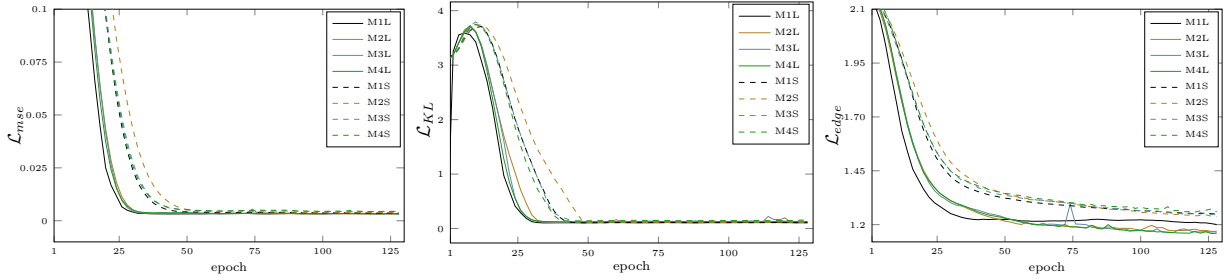
	$M1_t$	$M1_1$	$M2_t$	$M2_1$	$M3_t$	$M3_1$	$M4_t$	$M4_1$
# layers	10	10	12	12	15	15	17	17
# features	32	64	32	64	32	64	32	64

In Fig. 2 the losses evaluated on the validation dataset are shown. According to Fig. 2 the $M\#_1$ networks are faster and have better optimization process than the $M\#_t$: regarding the KLD all the network have similar performance, a slight gain is visible on the MSE and a bigger improvement is on the edge loss where $M4_1$ shows the best performance on both. It seems that deeper and wider network is able to better catch the properties of the image and to better filter the noise preserving spatial details.

3. EXPERIMENTS

In order to compare the performance of these architectures, we have carried out experiments on both simulated and real data. Numerical and visual results are shown. We select $(50 \times 256 \times 256)$ images from the simulated dataset and one real image from COSMO-SkyMed for testing. The networks listed in Tab.1 are trained for 130 epochs using the Adam optimizer [16] with learning rate $\eta = 0.0003$.

Fig. 2: Loss function evaluated on validation dataset, from left to right: Mean Square Error, Kullback-Leibler Divergence, Edge Loss. Dashed line correspond to $M\#_t$ features network. Solid to $M\#_1$ features network.



Tab 2 summarizes the numerical assessment on simulated and real data. Reference metrics, such as SNR, SSIM and MSE, are averaged on the full testing dataset. For assessment on real data we consider the M-index [17] that is a combination of the ENL and Haralick homogeneity. The ENL measures the ability of suppressing noise. The homogeneity quantifies left structures in the estimated noise, so give an indication on the ability of the filter in removing noise without suppressing useful information. In fact, pure speckle should be random and should not highlight no structures, producing an homogeneity equal to 0. So we decide to extract the homogeneity from M-index in order to highlight such behaviour of the filters.

Regarding simulated evaluation, Tab2 shows how wider ($M\#_1$) networks clearly outperforms the thinner ($M\#_t$) ones on all the index, with the only $M1_t$ having competitive results. This behaviour is totally in line with the validation loss. Among the wider networks $M3_1$ is the best one on all the index, even if all the solution are very close each other. In order to clearly evaluate the quality of the filter, visual inspection need to accompany the numerical consideration. In Fig.3, it is clear how all the $M\#_1$ are very close each other. It is important to notice that visually the best solution is $M4_1$ that shows a good edge preservation, while $M3_1$ and $M2_1$ tends to smooth and $M1_1$ presents small artefacts. Indeed, $M4_1$ is the solution that better reconstruct the antenna on the top of the storage tank (first clip) and better try to recover the lines of tennis pitch.

Fig. 3: Simulated results: detail of testing images selected by MercedlandUse dataset

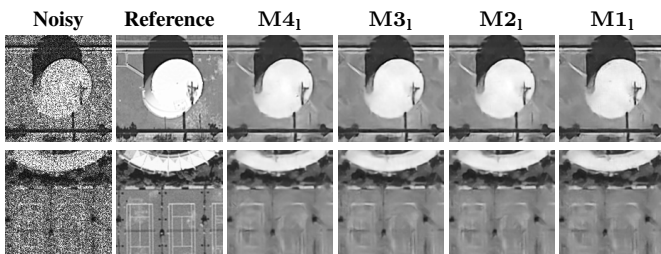


Table 2: Numerical results: on the left reference metrics for simulated images (SSIM, SNR, MSE); on the right no-reference metrics for real results (M-index, homogeneity (H)). Best value in blue, second best in red

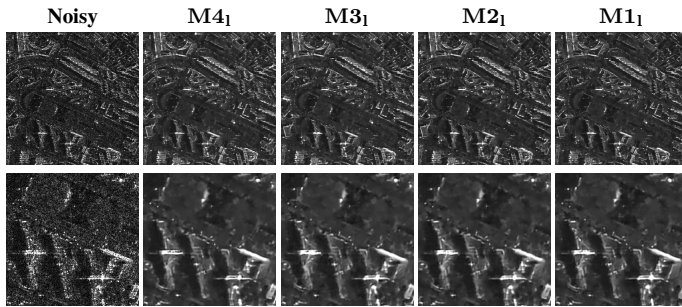
	SSIM	SNR	MSE	M-index	H(10^{-1})
$M1_t$	0.7279	8.2276	294	9.89	0.293
$M2_t$	0.7238	7.9600	311	10.47	0.276
$M3_t$	0.7180	7.4201	352	10.30	0.218
$M4_t$	0.7114	7.2222	366	8.76	0.117
$M1_1$	0.7344	8.3662	287	9.30	0.201
$M2_1$	0.7341	8.5677	273	8.29	0.139
$M3_1$	0.7389	8.6098	270	9.73	0.247
$M4_1$	0.7375	8.5635	272	7.46	0.003

When we are dealing with SAR images, assessment on simulated images is not enough because in simulation we can not include all the properties of a real SAR image. In order to have a full view of the performance of this filters, comparison on real SAR images is shown in Fig. 4. Also in this case, the solutions present very close results with slight differences. Observing the detail in the bottom of Fig.4, on homogeneous area all the filters produce very similar effect. the real difference is on the treatment of the objects that produce strong backscattering. Actually, the $M4_1$ is the solution that better preserve objects, while the other tend to smooth them making difficult the detection of single scatterers and impair the properties of adjacent areas. For comparison with other methods the reader is invited to refer to [14], where visual and numerical comparison of the $M1_1$ network with other method has been carried out.

4. CONCLUSION

In this work an analysis on the complexity of a network for SAR despeckling has been carried out. Starting from an our previous solution, we train different variations of the model changing its depth (number of layers) and width (number of features). As expected, deeper and wider networks perform

Fig. 4: Real results: on the top image of Naples from CosmoSky-Med, in the bottom a detail of the full image



better as long as the dataset fits with their complexity. Generally, even if there is not a big difference on the performance on simulated results, the deepest and widest network is the one that better can deal with real data. The bigger level of abstraction, the better generalization of the performance is ensured.

5. REFERENCES

- [1] F. Argenti, A. Lapini, T. Bianchi, and L. Alparone, “A tutorial on speckle reduction in synthetic aperture radar images,” *IEEE Geoscience and Remote Sensing Magazine*, vol. 1, no. 3, pp. 6–35, Sept 2013.
- [2] H. Aghababae, G. Ferraioli, G. Schirinzi, and M. R. Sahebi, “The role of nonlocal estimation in sar tomographic imaging of volumetric media,” *IEEE Geoscience and Remote Sensing Letters*, vol. 15, no. 5, pp. 729–733, May 2018.
- [3] Michele Ambrosanio, Fabio Baselice, Giampaolo Ferraioli, and Vito Pascazio, “Ultrasound despeckling based on non local means,” in *EMBECE & NBC 2017*, pp. 109–112. Springer, Singapore, 2017.
- [4] Antonio Mazza, Francescopaolo Sica, Paola Rizzoli, and Giuseppe Scarpa, “Tandem-x forest mapping using convolutional neural networks,” *Remote Sensing*, vol. 11, no. 24, 2019.
- [5] H. Aghababae, B. Kanoun, S. Vitale, and G. Ferraioli, “The use of nl paradigm in sar applications,” in *2019 IEEE 5th International forum on Research and Technology for Society and Industry (RTSI)*, Sep. 2019, pp. 120–123.
- [6] C. A. Deledalle, L. Denis, G. Poggi, F. Tupin, and L. Verdoliva, “Exploiting patch similarity for sar image processing: The nonlocal paradigm,” *IEEE Signal Processing Magazine*, vol. 31, no. 4, pp. 69–78, July 2014.
- [7] G. Ferraioli, V. Pascazio, and G. Schirinzi, “Ratio-based nonlocal anisotropic despeckling approach for sar images,” *IEEE Transactions on Geoscience and Remote Sensing*, vol. 57, no. 10, pp. 7785–7798, Oct 2019.
- [8] S. Vitale, D. Cozzolino, G. Scarpa, L. Verdoliva, and G. Poggi, “Guided patchwise nonlocal sar despeckling,” *IEEE Transactions on Geoscience and Remote Sensing*, vol. 57, no. 9, pp. 6484–6498, Sep. 2019.
- [9] Kaiming He, Georgia Gkioxari, Piotr Dollár, and Ross B. Girshick, “Mask R-CNN,” *CoRR*, vol. abs/1703.06870, 2017.
- [10] P. Wang, H. Zhang, and V. M. Patel, “Sar image despeckling using a convolutional neural network,” *IEEE Signal Processing Letters*, vol. 24, no. 12, pp. 1763–1767, Dec 2017.
- [11] G. Chierchia, D. Cozzolino, G. Poggi, and L. Verdoliva, “Sar image despeckling through convolutional neural networks,” in *2017 IEEE International Geoscience and Remote Sensing Symposium (IGARSS)*, July 2017, pp. 5438–5441.
- [12] S. Vitale, G. Ferraioli, and V. Pascazio, “A new ratio image based cnn algorithm for sar despeckling,” in *IGARSS 2019 - 2019 IEEE International Geoscience and Remote Sensing Symposium*, July 2019, pp. 9494–9497.
- [13] Giampaolo Ferraioli, Vito Pascazio, and Sergio Vitale, “A novel cost function for despeckling using convolutional neural networks,” *2019 Joint Urban Remote Sensing Event (JURSE)*, May 2019.
- [14] Sergio Vitale, Giampaolo Ferraioli, and Vito pascazio, “Edge preserving cnn sar despeckling algorithm,” *arXiv preprint arXiv:2001.04716*, 2020.
- [15] Yi Yang and Shawn Newsam, “Bag-of-visual-words and spatial extensions for land-use classification,” in *ACM SIGSPATIAL International Conference on Advances in Geographic Information Systems (ACM GIS)*, 2010.
- [16] Diederik P. Kingma and Jimmy Ba, “Adam: A method for stochastic optimization,” in *3rd International Conference on Learning Representations, ICLR 2015, San Diego, CA, USA, May 7-9, 2015, Conference Track Proceedings*, 2015.
- [17] Luis Gomez, Raydonal Ospina, and Alejandro C. Frery, “Unassisted quantitative evaluation of despeckling filters,” *Remote Sensing*, vol. 9, no. 4, 2017.